



# Rheological properties study of PBE, a random high impact polypropylene-based copolymer

Xingzhen Li<sup>1,2</sup> · Xiaoting Liu<sup>1,2</sup> · Xin Xie<sup>3</sup> · Chunli Liu<sup>1,2</sup> · Zhenbin Chen<sup>1,2</sup>  · Jixiong Kou<sup>1,2</sup> · Lei Wu<sup>1,2</sup> · Qianqian Chen<sup>1,2</sup>

Received: 10 May 2021 / Accepted: 26 July 2021 / Published online: 4 August 2021  
© The Polymer Society, Taipei 2021

## Abstract

In this work, rheological properties of a novel fabricated random high impact polypropylene-based copolymer, PBE, which possessed excellent properties of transparency and impact resistance, were studied. The studying included shearing stress, apparent shearing viscosity, viscous flow activation energy, extrudate swelling ratio, melt strength and melt extrusion morphology et al. The study was based on a capillary rheometer using RPB and RPE; both are used extensively at present, and the processing technologies are mature, as control. Based on the study, the following results arrived. Firstly, PBE is a pseudoplastic fluid and the processing methods used for RPE and RPB are fully applicable to PBE. Secondly, PBE presented the highest “shearing sensitivity” among above-adopted samples, and temperature and shearing rate showed the greatest influence on the rheological properties of PBE. Thirdly, the melt strength of PBE was significantly lower than that of RPB and RPE, but greatly varied with temperature, which indicated that injection molding was the most suitable for PBE. Finally, the study was also found that at a given shearing rate, the extruded swelling ratio of PBE was the smallest, which indicated this material has the best dimensional stability of the product.

**Keywords** Rheological properties · Study · Random high impact polypropylene-based copolymer · PBE · Capillary rheometer

## Introduction

After isostatic polypropylene (PP) was first polymerized and industrialized by Natta in the 1950s, materials prepared by PP have attracted fervent concern all over the world, and which made various products of PP entered many fields rapidly [1]. After more than 60 years development, products fabricated from PP have gradually been used in all aspects of people’s lives due to their excellent comprehensive performance, and make products such as woven products, injection molded products, films, tubes, etc. [2]. With the

development of the preparation technology of catalysts and PP production process, as well as the continuous growth of the global economic, the demand and consumption of PP are growing at a faster rate. In 2018, the global consumption of PP reached 67.81 million tons, of which the apparent consumption in China was 27.21 million tons, which accounted for 40% of the total global demand [3]. More importantly, the future growth degree of demand in China is still strong.

With the increasing performance requirements, some inherent defects of PP, such as low impact resistance, high haze and et al., are amplified gradually. To cater the higher and higher demand, modification studies are conducted extensively. At present, the modification research about PP is mainly focused only on one of above aspects, i.e., either enhancing the impact performance or improving the transparency, which, naturally led to the following results: PP with high impact performance showed low transparency, while with high transparency lacked good impact performance [12]. These defects greatly limited the expansion of the application of PP in both impact resistance and transparency [4]. Therefore, improving the overall performance of

✉ Zhenbin Chen  
zhenbinchen@163.com

<sup>1</sup> State Key Laboratory of Advanced Processing and Recycling of Nonferrous Metals, Lanzhou University of Technology, Lanzhou, Gansu 730050, China

<sup>2</sup> School of Material Science and Engineering, Lanzhou University of Technology, Lanzhou, Gansu 730050, China

<sup>3</sup> PetroChina Lanzhou Petrochemical Research Center, PetroChina, Lanzhou, Gansu 730060, China

PP to adapt to different application requirements become an urgent focus for the research about high-performance PP.

To meet the requirement for PP with both high impact resistance and low haze, the China Petroleum Lanzhou Chemical Research Center using a pilot plant for polypropylene with 75 kg/h Spheripol process by copolymerizing a certain amount of butene in the continuous phase of impact copolymerized PP using a double ring tube in series with a gas phase reactor. Through adjusting the quantities of butane, the refractive index between the continuous phase and the dispersed phase was regulated and controlled, and resulted in a product (named as PBE) that possessed high impact resistant and low haze simultaneously, which, exhibited a very robust application prospect naturally.

To provide a reasonable operation specification and further make this product in the actual application quickly, the processing properties must be first studied in detail because the known processing properties of various PP materials are different [5], and which meant that the mature processing method for other PPs is not necessarily satisfied to the production. Among all methods reported for the operation properties study, the Rheological study was adopted more because the results obtained can not only guide the synthesis of polymer with the excellent processing property, but also evaluate the processing performance, analyze the course of working, select the fabrication conditions, and direct the formula designing. Besides, the rheological study can also offer a reference for the design of processing machinery and mould [6].

Based on above reasons, the rheological properties of PBE were firstly studied by a capillary rheometer (RT2000, Gottfert, Germany) in this work, and the shearing stress, the apparent shearing viscosity, the viscous flow activation energy, the melt strength and the extrusion swelling ratio were explored, respectively, and the following results were obtained. Firstly, PBE exhibited similar rheological properties compared with those of known PPs. Secondly, with increasing of shearing rate the viscous flow activation energy of PBE decreased, and the corresponding melt viscosity is less sensitive to temperature, and so on. Finally, the rheological properties of PBE were further compared with propylene-butyl random copolymer PP (RPB) and ethylene-propylene-random copolymer PP (RPE), which has formed a mature processing scheme and the chain structure lay at the boundary of PBE to obtain the primary operation specification for its following fabrication and application. Firstly, it was found that the non-Newtonian index  $n$  of PBE has a greatly change with increasing temperature, indicating

**Table 1** Basic parameters of RPE, PBE and RPB

sample	MFR(g/10 min)	$M_w \times 10^{-4}$	$M_n \times 10^{-4}$	MWD
RPE	9.15	13	3.1	4.2
PBE	10.61	22.2	3.0	7.39
RPB	10.87	22.8	4.5	5.1

that the non-Newtonian nature of PBE is most dependent on temperature. Secondly, it was found that when the shearing rate increases, the viscous flow activation energy of RPE, RPB and PBE decreases in succession, indicating that the “shear-sensitivity” of PBE was higher.

## Experimental section

### Materials

Ethylene propylene random copolymer PP (RPE, RP260) was supported by China National Petroleum Corporation Lanzhou Petrochemical Branch. Random impact copolymer PP (PBE) and propylene-butyl random copolymer PP (RPB, RPB08D-2) were provided by PetroChina Lanzhou Chemical Research Center. Parameters, such as melt flow rate, the molecular weight and the molecular weight distribution, of above polymer were determined, and results were shown in Table 1. The antioxidant 1010 ( $\geq 98\%$ ) and antioxidant 168 ( $\geq 99\%$ ) was purchased from BASF SE, Germany. Calcium stearate (40–97%) was purchased from Hebei Qian You New Material Technology Co.

### Sample preparation

Antioxidant 1010, antioxidant 168 and calcium stearate were added to RPB, RPE and RPB at a mass ratio of 0.05 wt%, 0.1 wt% and 0.04 wt%, respectively, and then co-mixed at high speed in a high-speed mixer (GRH100, Fuxin Hong Qi, Plastic Machinery Factory) for 5 min. After that, the three mixtures were granulated by a twin-screw extruder (ZSE-34, Rice, Germany) under the parameters showing in Table 2, and the related master batches were obtained.

### Characterization of the rheological properties

15 g of above-prepared master batch were introduced into a capillary rheometer (RT2000, Gottfert, Germany) which was fitted with a mouth mold with the length-diameter ratio

**Table 2** Processing parameters of twin screw extruder

Barrel temperature (°C)					Screw speed(rpm)	Feeder speed(rpm)	Pelletizer speed(rpm)
T <sub>1</sub>	T <sub>2</sub>	T <sub>3</sub> -T <sub>7</sub>	T <sub>8</sub>	T <sub>9</sub>			
140	160	190	160	150	120	25	25

**Table 3** Shearing rates corresponding to different stages

Paragraphs	1	2	3	4	5	6	7	8	9
Shearing rate( $s^{-1}$ )	90	180	202.5	303.75	455.634	683.442	1025.15	1537.74	2306.61

of 30:1, and the test temperature was then set to 160 °C. After the temperature was raised to the set temperature and kept constant for 3 min, the rheological performance experiments were started at the set shearing rate, where the shearing rate was set as shown in Table 3. Finally, the above steps were repeated at test temperatures of 170 °C, 180 °C, 190 °C, 200 °C, 210 °C and 220 °C, respectively.

### Characterization of the melt tensile rheological properties

Firstly, the capillary rheometer (RT2000, Gottfert, Germany) orifice die length-to-diameter ratio, test temperature, melt extrusion rate, roller acceleration and tensile length were set to 20:1, 160 °C, 11.3 mm/s, 6 mm/s and 110 mm, respectively. Then 15 g of the above prepared sample was added to the capillary rheometer which was allowed to rise to the set temperature and maintained for three minutes to conduct the experiment. Finally, the above steps were repeated at test temperatures of 170 °C, 180 °C, 190 °C and 200 °C, respectively.

### The melt extrusion swelling ratio characterization of PBE

The RT2000 capillary rheometer was still used to investigate the melt extrusion expansion ratio at 170 °C, 190 °C and 210 °C, respectively. First, the orifice die length-to-diameter ratio and melt extrusion rate of the capillary rheometer were set to 30:1 and 11.3 mm/s, respectively. And then 15 g of the above samples were added to the capillary rheometer, when the temperature was raised to the set temperature with a constant temperature for three minutes, the IR detector was turned on to investigate the melt extrusion expansion ratio.

## Results and discussion

### Rheological performance of PBE

#### Relationships among shearing stress, temperature and shearing rate

The relationship among shearing stress( $\tau$ ), temperature (T) and shearing rate ( $\dot{\gamma}$ ) were shown in Fig. 1. Obviously, with the increase by shearing rate, the shearing stress increased continuously, but the increased degree was decreased gradually. However, the shearing stress decreased with the rising of temperature. The above phenomenon could be ascribed

to the structural alteration of the flow system. Different from the flow system formed from the low molecular compounds, the structure of the polymer flow system would change obviously with the variation of shearing rate and temperature because the entanglement structure and the crystalline texture varied greatly with them, and  $\tau$  varied with the variation  $\dot{\gamma}$  and T naturally [28]. For  $\dot{\gamma}$ , as it was exerted to polymer melt, the old entanglement structure and crystalline texture would be destroyed. In contrast, the new entanglement structure and the crystalline texture could not form because the formation of them lagged behind its the destroy greatly, which would decrease amounts of entanglement structure and crystalline texture, thus, the interaction between the different flow layers diminished, and resulted in the decrease of viscosity. With the increasing of  $\dot{\gamma}$ , the entanglement structure and the crystalline texture would be destroyed at a larger degree, the interaction between the adjacent layers decreased at a larger degree, which would decrease the viscosity at a large degree, and further result in has a greatly decreased of  $\tau$ . What's more, the increased  $\dot{\gamma}$  meant the movement acceleration, according to the second Newton's law, greater force would be demanded to overcome the internal friction, thus,  $\tau$  would show an increased value. Just for the cooperation of above two aspects, the shearing stress increased continuously, but the degree of increasing was decreased gradually. As for T, the elevation of it would enlarge the volume of polymer melt, which would increase the distance between two adjacent layers, and resulting in the decrease of the interaction force, the viscosity decreased correspondingly, and  $\tau$  decreased naturally. Besides, the increase of

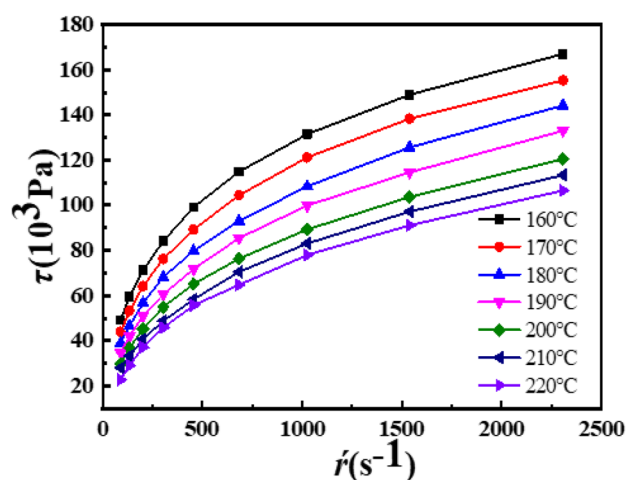


**Fig. 1**  $\tau$ - $\dot{\gamma}$  curves of PBE at different temperatures

temperature would increase the kinetic energy of all movement units in the polymer [8], which would make the entanglement structure and the crystalline texture be destroyed easily, and the interaction between the different layers would be weakened correspondingly, and further resulted in the decreased  $\tau$  accordingly.

To further verify explanation obtained from us and to find the deviation degree of this novel product to the Newtonian fluid law, Eq. (1) was adopted to the following further analysis:

$$\tau = K\dot{\gamma}^n \quad (1)$$

where, K stood for the consistency factor, n was a power, it reflected the fluids kind, and further explore it could obtain the deviation degree of the fluids to the Newtonian fluids.

Taking the logarithm from both side, and Eq. (2) was obtained.

$$\lg\tau = \lg K + n\lg\dot{\gamma} \quad (2)$$

Plotting  $\lg\tau$  against  $\lg\dot{\gamma}$ , from which we could get the value of n from the slope and K from the intercept. After comparing n with 1, the kind and the deviation degree of fluids to the Newtonian fluids could be obtained [11].

From Fig. 2, it could be found that the logarithm value relationship between shearing stress and shearing rate was linearly correlated at each temperature, which indicated that the rheological behavior of the PBE melt in the experimental temperature range in accord with the power-law equation.

From the n-value, K-value and linear correlation coefficient R in Table 4, it could be further obtained that the rheological behavior of the PBE melt conformed to the power-law equation, and PBE polymer was a typical pseudoplastic fluid, which indicated that similar processing method with the commercial PP might be used to PBE.

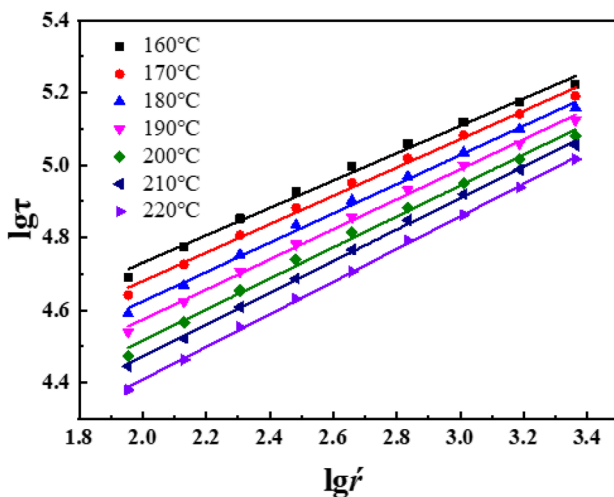


Fig. 2  $\lg\tau$ - $\lg\dot{\gamma}$  curves of PBE at different temperatures

**Table 4** Non-Newtonian index and consistency coefficient of PBE at different temperatures

Temperature(°C)	<i>n</i>	Correlation coefficient <i>R</i>	<i>K</i> (Pa · s)
160	0.3778	0.9967	9444
170	0.3913	0.9973	7903
180	0.4034	0.9983	6573
190	0.4141	0.9986	5574
200	0.4269	0.9976	4601
210	0.4367	0.9993	3975
220	0.4497	0.9959	3235

### Relationships among shearing viscosity, temperature and shearing rate

To evident our thoughts about the shearing viscosity of PBE would decrease with the increase of temperatures and shearing rate, relationships among shearing viscosity, temperature and shearing rate were shown in Fig. 3. It obviously exhibited with the increase of shearing rate, shearing viscosity decreased rapidly at first and then tended to flatten, which indicated our previous analysis about the lag of formation of entanglement structure and crystalline texture to them destroy the resulting amount of them decrease. The lag of entanglement structure formation could be attributed the following reasons: The first was viscosity. Due to the high molecular weight of the polymer, the interaction between any two adjacent molecular chains was large because lots of weak interaction sourced from the van der Waals' force would add to each other and produce a very large force, which would make the relative slippage between them difficult. Besides, the orientation of molecular chains was another reason. Macromolecules under shearing conformational would change, and the tangled chains

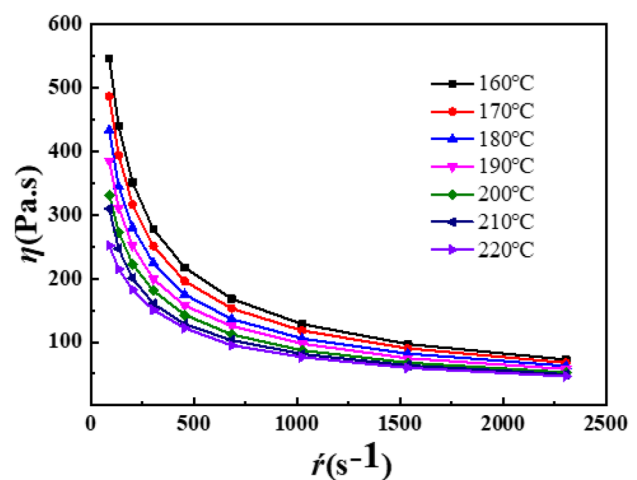


Fig. 3  $\eta$ - $\dot{\gamma}$  curves of PBE at different temperatures

began to untangle and orientate along the direction of flow [19], which would make them stretch, the probability of entanglement decreased. With the increasing shearing rate, untangling speed and orientating degree of polymer chains increased, while the entangling probability decreased correspondingly. Whereas the lag of crystalline texture formation could be ascribed to the high viscosity, the relative slippage among chains and the low stability of the primary crystal nucleus. Due to the high viscosity, the neat arrangement of chain segments in polymer either into lattices that had formed or to form new lattices would become difficult and Time-consuming, which made the formation of crystalline texture difficult under the quicker slippage of chains, added to the low stability of primary crystal nucleus, the quantity of novel formed crystalline texture in a short time would be much smaller than that of the destroyed.

When the test temperature was higher than  $T_g$  by 100 °C, *i.e.*,  $T > T_g + 100$  °C, the free volume in the polymer melt would be very large [13]. The magnitude of the fluid viscosity critically depends on the structure of the polymer molecular chain itself [7]. At this condition, the Arrhenius equation would be satisfied, and the relationship between the polymer melt viscosity  $\eta$  and the temperature  $T$  could be expressed as Eq. (3).

$$\eta = Ae^{\Delta E/RT} \quad (3)$$

where  $A$  represented the coefficient related to the viscosity of the material.  $R$  was the gas constant.  $\Delta E$  stood for the activation energy of the viscous flow.

Taking the logarithm from two sides of the equation, and a novel Eq. (4) was obtained. Through this equation, the activation energy of viscous flow could be calculated.

$$\ln\eta = \ln A + \frac{\Delta E_\eta}{RT} \quad (4)$$

Plotting curves of  $\ln\eta$  against  $1/T$  from the above experiment data, and results of the sample under different shearing rates were shown in Fig. 4 and Table 5.

From them, we could obtain that values of the linear correlation coefficients for each curve was bigger than 0.99, which indicated a good linear relationship between  $\ln\eta$  and  $1/T$ , and also documented that the apparent viscosity and temperature of PBE under all tested shearing rates were accord with the Arrhenius equation. Besides, results also presented that the viscous flow activation energy was decreased with the increasing shearing rate. First of all, the viscous flow activation energy was the minimum energy value of flow units (or chain segments in the case of polymers) required to overcome a barrier and moved from their original position to a nearby "cavity" in the melt flow [9]. This value not only reflected the ease of flow, but also the temperature sensitivity of the viscosity of the material. The viscous flow activation energy of PBE decreased with the increasing shearing rate at the set temperature could be mainly ascribed to the shear-induced variation of the molecular state. When the shearing stress was applied from outside, the entanglement between polymer chains would be weakened, and the ability of movement would become

**Fig. 4**  $\ln\eta$ - $1/T$  curves of PBE at different shearing rates

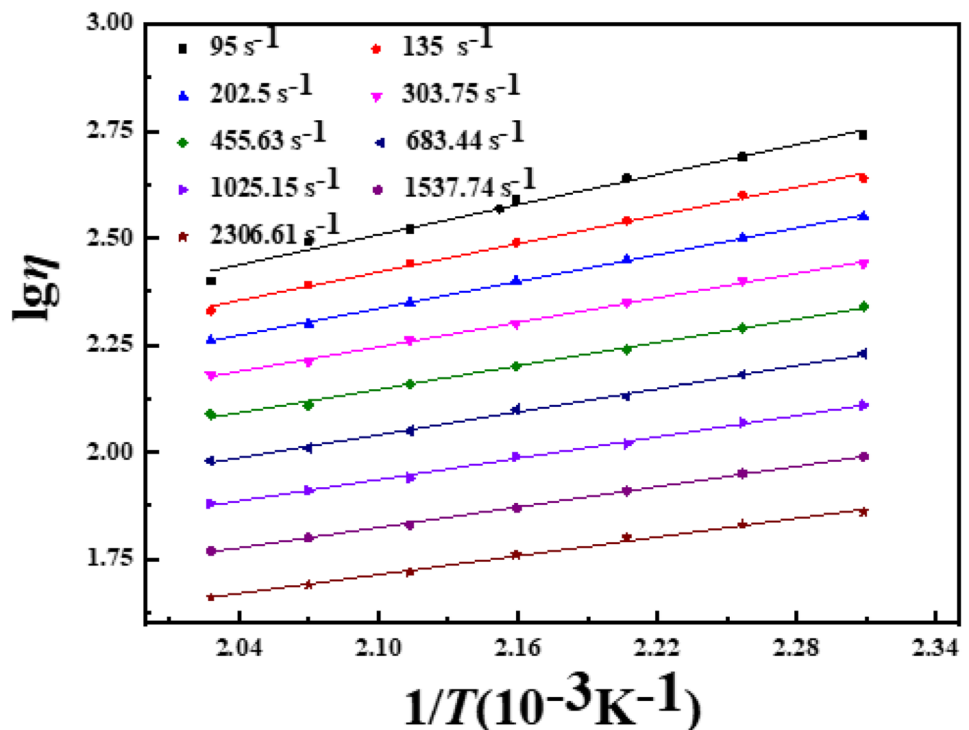


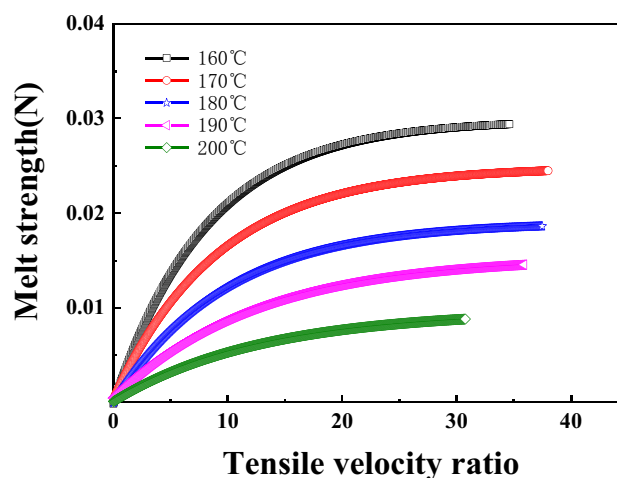
**Table 5** Viscous flow activation energy of PBE at different shearing rates

$\dot{\gamma}(\text{s}^{-1})$	Correlation coefficient $R_2$	$\Delta E_{\eta}(\text{KJ}\cdot\text{mol}^{-1})$
90	0.9930	22.13
135	0.9996	21.04
202.5	0.9995	19.65
303.75	0.9998	18.67
455.634	0.9982	17.71
683.442	0.9995	17.18
1025.15	0.9983	15.98
1537.74	0.9985	15.07
2306.61	0.9984	13.69

easy [22]; added to the orientation function of molecular chains, the free space in polymer melt became larger, which would also improve the movement ability of the chain segment. Just for the above two-aspect reasons, a decrease for the activation energy of viscous flow could be understood reasonably, the temperature sensitivity of the corresponding melt viscosity of PBE was also gradually decreasing.

#### Effect of tensile ratio on the strength of PBE melt

Melt strength was an index from which whether a polymer melt can support its weight could be evaluated [14]. It was an important parameter in many processes, such as extrusion coating, blow molding, profile extrusion, thermoforming and foaming et al. So, the study about the relationship between melt strength and tensile velocity ratio was conducted and a graph of the relationship between the melt strength of the sample and the tensile velocity ratio (the ratio of the instantaneous rate of the melt tensile rheometer roller to the initial rate) was obtained, and the result was shown in Fig. 5. It could be found that the trend of the curve could be divided into two parts: the rising region and the platform region. The change of melt strength is mainly caused by the interaction among molecular chains in the polymer matrix [10]; under the low tensile velocity ratio, polymer molecular chains were stretched. Under this condition, the interaction force increased rapidly along a direction of polymer chains regular arrangement, and its melt strength also increased dramatically. Moreover, when the tensile velocity ratio increased to a certain extent, the orientation of polymer molecular chains became nearly the same, the distance between the molecular chains would hardly change, the force would gradually remain to a constant nature, and the increasing degree of the melt strength also decreased to a constant gradually. In other words, the “strain hardening” would stop the increase of the melt strength. Figure 5 also presented that the increase of temperature would decrease the melt strength

**Fig. 5** The relationship between melt strength and tensile speed ratio of PBE at different temperatures

of PBE, *i.e.* as temperature increased gradually from 160 °C to 200 °C, the melt strength decreased gradually from 0.03 N to 0.005 N, and which could be ascribed to the cooperation effect of kinetic energy and the free volume. With the increase of temperature, the kinetic energy of each moving unit in the PBE molecule increased, added to the distance increasing between the adjacent molecular chains sourced from the increased free volume, the interaction among molecules weakened, which would result in the decrease of melt strength naturally [23]. Besides, the results of this experiment documented that the method using lower temperature to enhance the melt strength of PBE during processing was a simple and effective way.

#### Extruded swelling ratio of PBE

Extrusion expansion of the melt, also known as extrusion swelling or the Barras effect, is a phenomenon in which the cross-sectional area of the extrudate is larger than the cross-sectional area of the membrane pore after the melt extruding [21]. From a macro-rheological point of view, extrusion swelling is a parameter related to the elasticity of the polymer melt [27]. It is the result of the recovery of the elastic deformation of the sample. This phenomenon affects the quality of the extruded product, the extrusion process, even the design of the extrusion dies and head. Therefore, it is necessary to investigate the extrusion swelling behavior of PBE under different extrusion conditions because it can provide theoretical support for the processing conditions of PBE.

Figure 6 showed the trend of the extrusion expansion ratio of the melt with a shearing rate under different temperatures (in which PBE was tested with a capillary rheometer with  $L/D = 30/1$ ). It could be found that as the pore aspect ratio

was fixed, the extrusion expansion ratio increased gradually with the increase of shearing rate. When the shearing rate increased to a certain extent, the increasing degree of extrusion expansion ratio decreased slowly and tended to a constant, which could be attributed to the orientation of chains and segments of polymer. With the increase of pre-shearing rate, the shearing stress increased, the chains and segments in polymer melt would get an orientation form along of the exerted force, thus, more and more elastic energy would be stored. In addition, due to the increase of shearing rate, the flow time of the melt in the mouth and mold would be shortened gradually [26], which would result in the relaxation probability of molecular chains and segments that had been oriented decreasing relatively. The cooperation of the above factor would make the stored elastic energy increased persistently. After leaving the mouth of the mold, the elastic energy stored in molecular chains and segments would be released with an explosive method, and the oriented chains and segments would return to the stable state, again, which would result in the increasing of extrusion swelling ratio accordingly. At a later stage, when the shearing rate increased to a certain level, the chain segments of the polymer molecules would arrive at a complete orientation gradually, the elastic energy they stored would increase to the limitation gradually, and the export expansion ratio would gradually increase to a constant naturally.

Besides, Fig. 6 also presented the extrusion expansion ratio of the melt decreased to about 14% when the temperature increased from 170 to 210 °C at the same shearing rate, which could be attributed to the increased movement ability of molecular chains and segments. With the rising of temperature, both the free volume of polymer matrix and the kinetic energy of polymer chains would increase [29], which would be facilitated to the disorientation of polymer, and

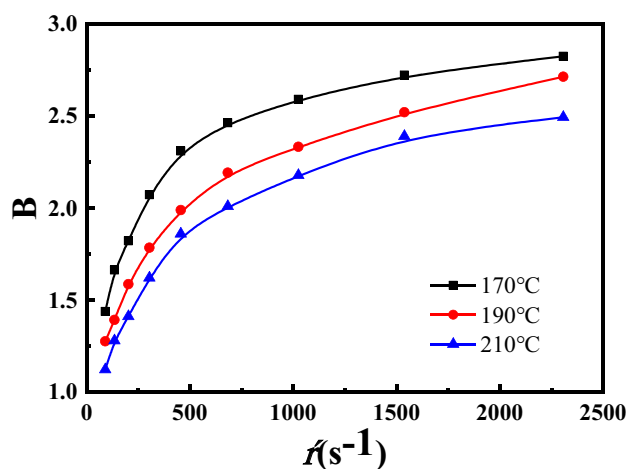


**Fig. 6** The relationship between the extrusion expansion ratio and shearing rate of PBE at different temperatures

the produced elastic energy from the shearing flow during extrusion would be released easily. As a result, a decreased extrusion swelling ratio could be observed. Based on this result, it could be concluded that increasing the temperature to decrease the extrusion expansion of PBE and ensure the accuracy and stability of the dimensions of the product to be possible.

### Comparative analysis of the rheological properties of PBE, RPE and RPB

Due to the structural differences among different types of PP's copolymer, the rheological properties of the melt would not be the same naturally [30], thus, the processing conditions for each PP should exist some difference. In order to obtain more accurate processing boundary conditions, one was ethylene propylene random copolymer PP (RPE, RP260), the other was propylene-butyl random copolymer PP (RPB, RPB08D-2), were conscripted as a control to get a further study to provide more feasible support for the processing of PBE. The reasons for adopting them was that they presented similar fusing fingers with PBE, and the processing process had matured. Besides, the monomer composition of the above two samples stayed at the two limitation boundary sides of PBE.

### Effect of shearing rate on the rheological properties of PBE, RPE and RPB

As shown in Fig. 7, the shearing stress for both RPE and RPB was increased gradually with the increase of the shearing rate or the decline of temperature, which were consistent with the rheological behavior of PBE. However, it could be observed that at the same shearing rate or temperature, the shearing stress of PBE and RPB were significantly lower than that of RPE, the reason could be ascribed to the composition difference of polymers. The copolymerized monomer for PBE and RPB was 1-butene, while the copolymerized monomer of RPE was ethylene; because the steric resistance produced by 1-butene was higher than that of ethylene, the average distance between two adjacent polymer chains for PBE and RPB was larger than that of RPE under the same conditions. Because the attraction between molecules would decrease with the distance [31], a weaker intermolecular interaction in PBE and RPB matrix would be produced naturally. Besides, the increase of distance between two adjacent molecules chained would also decrease the tangling probability among them, which would also lead to the decrease of the interaction force at a whole state and result in lower shearing stress correspondingly.

The relationship between  $lgt$  and  $lg\dot{\gamma}$  for RPE, PBE and RPB at different temperatures were shown in Fig. 8 and Table 6. From Fig. 8, a well linear relationship between

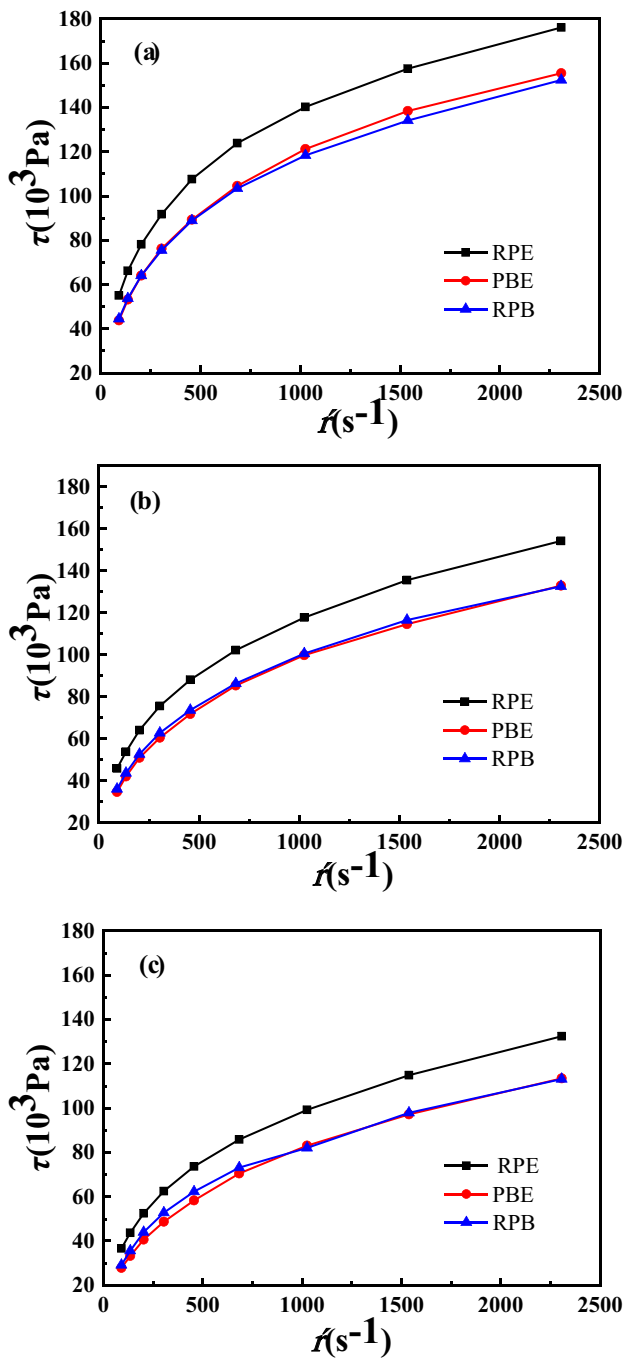


Fig. 7  $\tau$ - $\dot{\gamma}$  curves of PBE, RPE and RPB at different temperatures (a) 170 oC; (b) 190 oC; (c) 210 °C

$lg\tau$  and  $lg\dot{\gamma}$  for three samples was observed. From Table 6, it could be found that the correlation coefficients ( $R^2$ -values) for RPE, PBE and RPB were all exceeded than 0.99 at given experimental temperature, which also documented that  $lg\tau$  and  $lg\dot{\gamma}$  possessed a well linear relationship. Secondly, n-values for PBE, RPB and RPE showed a sequentially decreasing trend in the given experimental

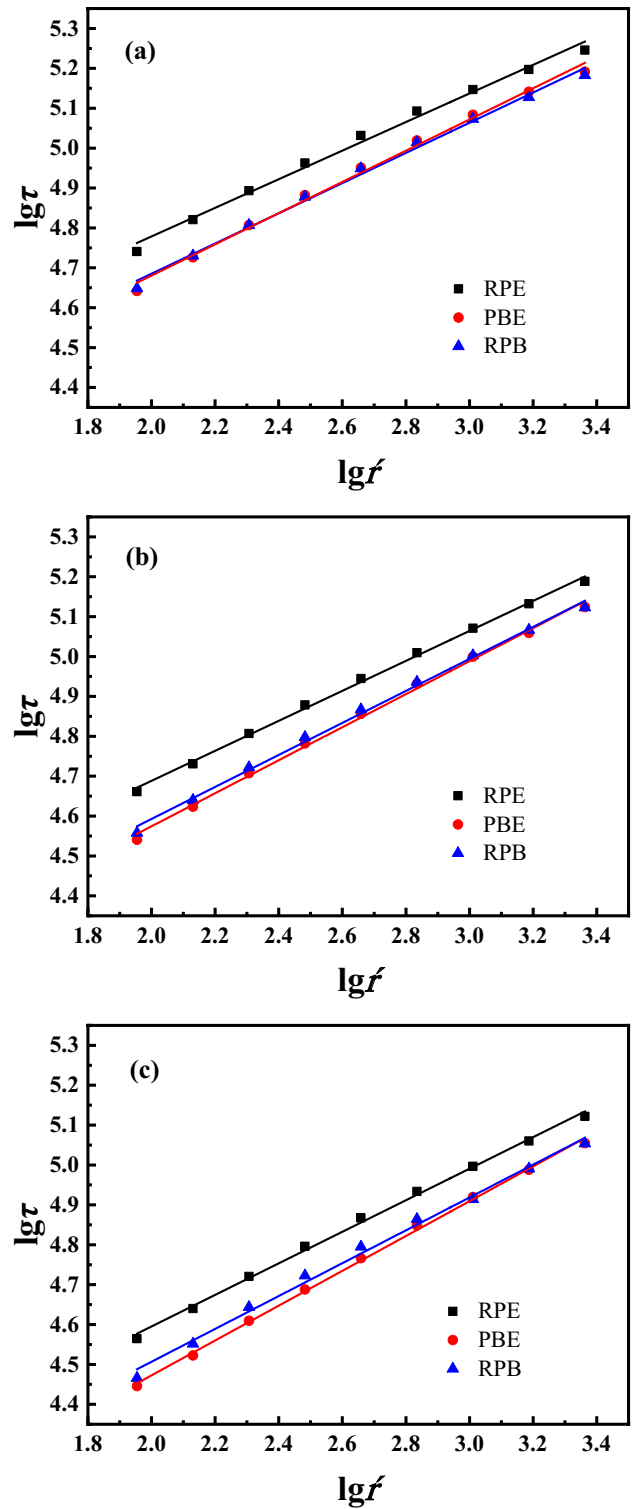


Fig. 8  $lg\tau$ - $lg\dot{\gamma}$  curves for PBE, RPE and RPB at different temperatures (a) 170 oC; (b) 190 oC; (c) 210 oC

temperature, while the K-values changed in an opposite pattern. The value of n indicated that the non-Newtonian order of the three samples was RPE > RPB > PBE. This



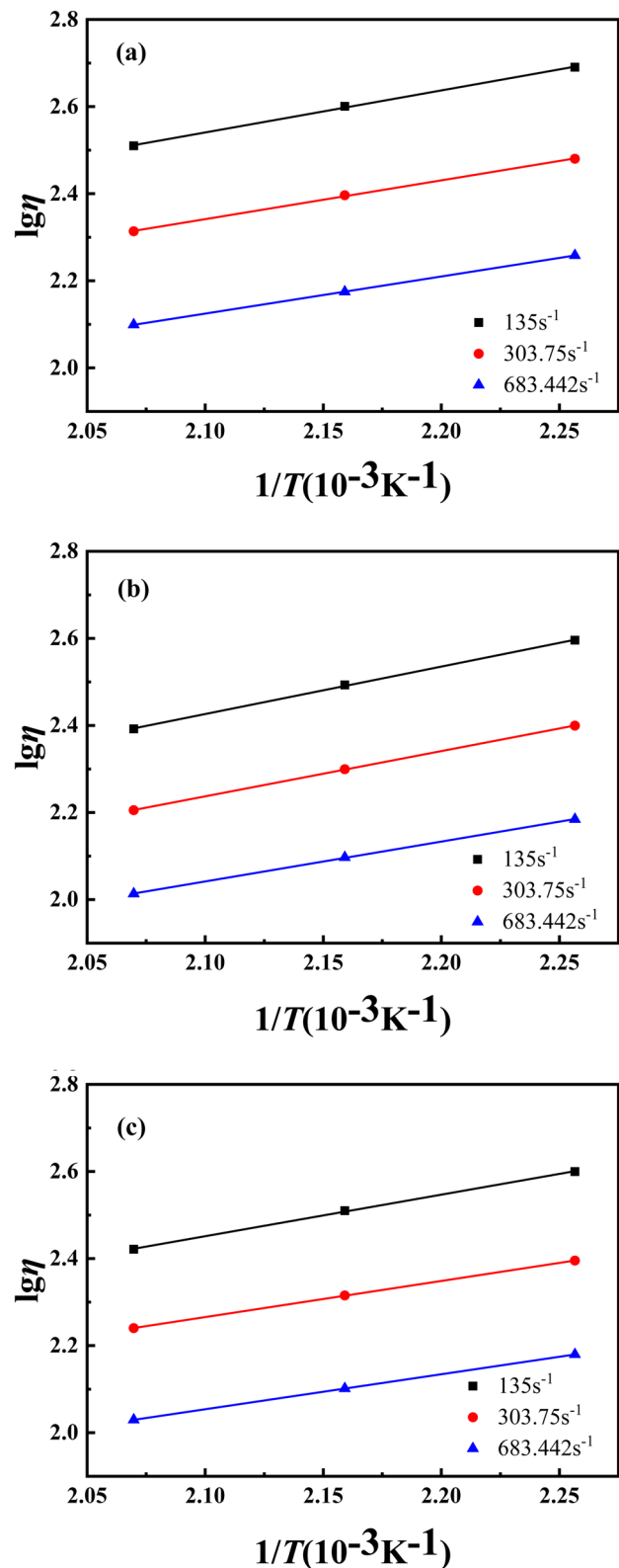
**Table 6** Non-Newtonian exponents and consistency coefficients of PBE, RPE and RPB at different temperatures

sample	Temperature (°C)	Correlation coefficient $R^2$	$N$	$K$ (Pa · s)
RPE	170	0.9965	0.3585	12,334
	190	0.9989	0.3759	9125
	210	0.9988	0.3955	6701
PBE	170	0.9973	0.3913	8022
	190	0.9986	0.4141	5899
	210	0.9993	0.4367	4175
RPB	170	0.9997	0.3785	8520
	190	0.9986	0.4013	6574
	210	0.9993	0.4119	5086

phenomenon was also caused by the variation in the chain structure of the three materials. Firstly, due to the different types of copolymer monomer, the steric resistance of RPB and PBE was higher, which would increase the distance between the adjacent molecular chains, and result in a lower probability of chain entanglement. The lower entanglement among molecule chains meant the entangled structure could be destroyed more rapidly and easily [17]. In contrast, the large distance meant the formation of new entangled structure became more hardly and slowly. Because the non-Newtonian nature was mainly sourced from the entangling among molecule chains [24], the small entangle number would result in high Newtonian nature naturally. The difference in  $n$  value of PBE and RPB could be attributed to the difference in molecular weight and molecular weight distribution. Compared the molecular weight distribution, we could find out both  $PDI$  and  $M_n$  of PBE was wider and smaller than that of RPB, which meant there were a large amount of low molecular weight molecules in PBE. Because the small molecules could play the role of plasticizer, the Newtonian of PBE would increase [20]. What's more, the existence of small molecules could increase the distance among large molecules, the probability and degree of entanglement would decrease [25], which would also increase Newtonian of PBE. All in all, the highest  $n$  of PBE at the same temperature and shearing rate documented its flow stability was best.

#### Effect of temperature on the activation energy of PBE, RPE and RPB

The shearing viscosities of RPE, PBE and RPB at 170 °C, 190 °C and 210 °C under different shearing rate were presented in Fig. 9. Because the processing temperature was one of the most important ways to regulated polymer fluidity

**Fig. 9**  $\eta$ - $\dot{\gamma}$  curves of PBE, RPE and RPB at different temperatures (a) 170 °C; (b) 190 °C; (c) 210 °C

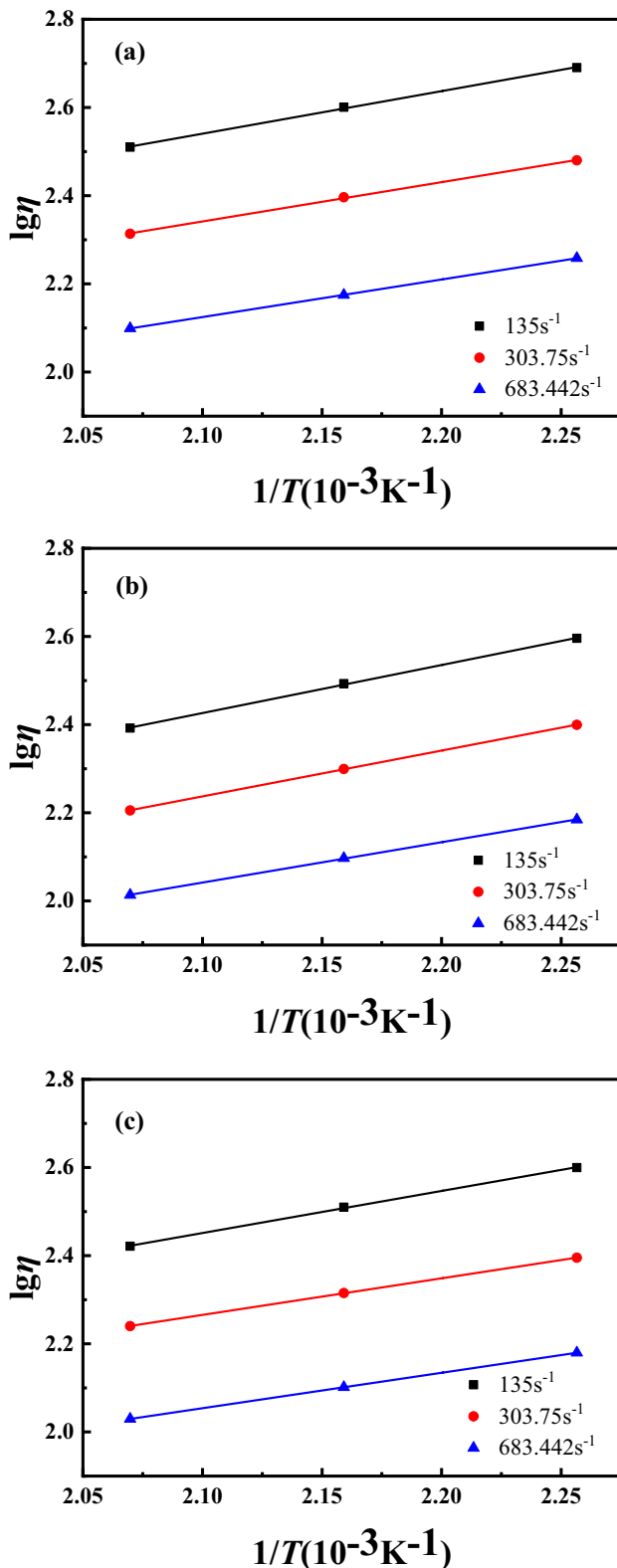


**Fig. 10**  $\ln\eta$ - $1/T$  curves of PBE, RPE and RPB at different shearing rates (a) RPE; (b) PBE; (c) RPB

[18], and the sensitivity of viscosity to temperature varied for various polymers, investigation of the sensitivity of viscosity to temperature would be necessary. Besides, because the shearing rate used in the actual production was always set in the range of  $10^2$ - $10^3$   $s^{-1}$ ,  $\dot{\gamma}$  in the experiment was chosen as  $135$   $s^{-1}$ ,  $303.75$   $s^{-1}$  and  $683.442$   $s^{-1}$  to compare the viscous flow activation energy of RPE, PBE and RPB, making the theoretical study more suitable for the practical application. The relationship between  $\ln\eta$  and  $1/T$  for the three samples at different shear rates was plotted according to the Arrhenius equation, and results were shown in Fig. 10. The viscous fluid activation energy  $\Delta E$  were shown in Table 7. It could be seen that the viscous flow activation energy  $\Delta E$  of PBE was the highest at the same shearing rate, which meant the viscosity of PBE was more sensitive to temperature than that of RPE and RPB, and it was easier for PBE to regulate its flowability by increasing the temperature during processing.

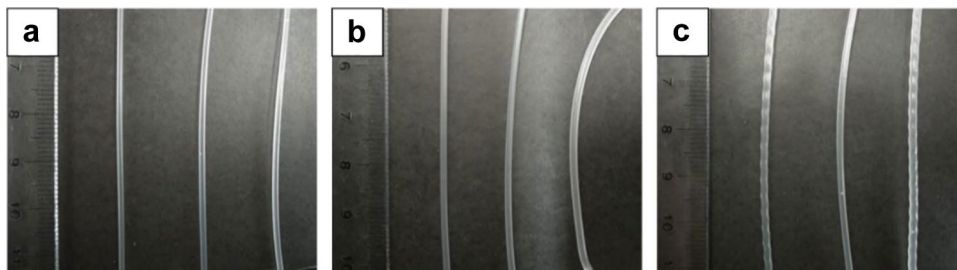
#### Comparison of the extruded morphology of PBE, RPE and RPB

The morphology of extrudate for three samples at different shearing rates was investigated to ensure the accuracy and stability of the product dimensions in the actual production, and results were shown in Fig. 11. It could be found out that at lower shearing rates, the extrudates of PBE, RPE and RPB displayed a smooth morphology. Because low shearing rate meant polymer had enough time to adjust the changed conformation of their chains as passing through the mouth die [15]. However, as the shearing rate increased, RPE and RPB showed unstable flow gradually, and clear threads appeared, while the melt extrusion morphology of PBE remained smooth. The reason for this phenomenon could be ascribed to the fact that PBE possessed a wider molecular weight distribution and a smaller molecular weight. Because wider molecule weight distribution and low molecule weight meant there were a large number of small molecular weight polymer [16], which would increase the distance between two adjacent polymer chains, and decrease the entanglement degree among different chains, and further decrease

**Table 7** Viscous flow activation energies of PBE, RPE and RPB at different shearing rates

$\dot{\gamma}(s^{-1})$	$R_2$			$\Delta E_{\eta}(KJ \cdot mol^{-1})$		
	RPE	PBE	RPB	RPE	PBE	RPB
135	0.9996	0.9998	0.9998	18.48	20.88	18.28
303.75	0.9998	0.9998	0.9999	17.06	19.90	15.89
683.442	0.9999	0.9995	0.9999	16.32	17.53	15.39

**Fig. 11** Extrusion morphology of RPE, PBE and RPB at different shearing rate (a)  $135\text{ s}^{-1}$ ; (b)  $303.75\text{ s}^{-1}$ ; (c)  $683.442\text{ s}^{-1}$



the stored elastic energy, thus, the stored elastic energy in extrusion could be more and more easily dissipated after it departing the mouth of the model, and finally made the extruded sample showing the smooth shape remained at a higher shearing rate. This result documented that PBE possessed a more extensive shearing rate range than that of RPE and RPB.

## Conclusion

PBE was a typical pseudoplastic fluid, and the viscous activation energy of PBE would be reduced with the increasing of shearing rate, and the temperature sensitivity of PBE was high. The extrusion swelling phenomenon occurred when the PBE melt was extruded from the mouth die at high shearing rate, and the extrusion swelling ratio increased first and then stabilized, while the extrusion swelling ratio of PBE was effectively reduced by increasing the temperature. After compared with RPE and RPB, we found that the non-Newtonian of PBE was the smallest, but it changed the most with the increase of temperature. Besides, the shape of PBE sample remained smooth even at higher shearing rates, while RPE and RPB showed "threads", and demonstrated that PBE possessed a larger adjusting range of temperature and shearing rate than RPE and RPB in the molding process of production.

**Acknowledgements** This work was supported by the National Natural Science Foundation, China (Grant: 51061009), the Innovation and Entrepreneurship Talent Project of Lanzhou (2019-RC-53), and the Innovation Foundation of China National Petroleum Corporation(2019D-5007-0408).

## References

- Wang S, Chen K, Jia M (2019) Effect of processing conditions on the microstructure of microcellular PP/WF composites prepared by the continuous extrusion molding technology. *Materials Research Express* 7(1):015308
- Koffi A, Koffi D, Toubal L (2020) Mechanical properties and drop-weight impact performance of injection-molded HDPE/birch fiber composites. *Polymer Testing* 93:106956.
- Liu G, Jia F, Yue Q (2016) Decoupling of nonferrous metal consumption from economic growth in China. *Environ Dev Sustain* 18(1):221–235
- Schäferling M, Häfner B, Lanza G (2019) Effects of defects in hybrid sheet moulding compound—Evaluation of defects and the impact on mechanical properties. *Materialwiss Werkstofftech* 50(11):1317–1325
- Ye X, Ma S, Jiang X (2019) The adsorption of acidic gaseous pollutants on metal and nonmetallic surface studied by first-principles calculation: A review. *Chin Chem Lett* 30(12):2123–2131
- Mishra JK, Hwang K-J, Ha C-S (2005) Preparation, mechanical and rheological properties of a thermoplastic polyolefin (TPO)/organoclay nanocomposite with reference to the effect of maleic anhydride modified polypropylene as a compatibilizer. *Polymer* 46(6):1995–2002
- Roh EJ, Kim JM, Baig C (2019) Molecular dynamics study on the structure and relaxation of short-chain branched ring polymer melts. *Polymer* 175:107–117
- Rey-Stolle M, Fernández-Martín F, Tagle L (1998) Some properties of poly (carbonates) and poly (thiocarbonates) from diphenols with methyl groups in the 3-position in the phenyl rings. *Polym Int* 46(2):93–98
- Morioka S, Sun M-H (2009) Evaluation of the activation energy of viscous flow in the dense gas-like model. *J Non-Cryst Solids* 355(4–5):287–294
- Hwang SY, Yoo ES, Im SS (2012) The synthesis of copolymers, blends and composites based on poly (butylene succinate). *Polym J* 44(12):1179–1190
- Ibrahim S, Nienow A (1999) Comparing impeller performance for solid-suspension in the transitional flow regime with Newtonian fluids. *Chem Eng Res Des* 77(8):721–727
- Aulin C, Karabulut E, Tran A (2013) Transparent nanocellulosic multilayer thin films on polylactic acid with tunable gas barrier properties. *ACS Appl Mater Interfaces* 5(15):7352–7359
- Wang D, Wang J (2021) A sensitive and label-free electrochemical microRNA biosensor based on Polyamidoamine Dendrimer functionalized Polypyrrole nanowires hybrid. *Microchim Acta* 188(5):1–10
- Foss PH, Tseng HC, Snawerdt J (2014) Prediction of fiber orientation distribution in injection molded parts using Moldex3D simulation. *Polym Compos* 35(4):671–680
- Wang T, Coropceanu V, Brédas J-L (2019) All-polymer solar cells: impact of the length of the branched alkyl side chains on the polymer acceptors on the interchain packing and electronic properties in amorphous blends. *Chem Mater* 31(16):6239–6248
- Baranwal K, Jacobs HL (1969) Effect of mastication on molecular weight and molecular weight distribution of EPDM polymer and SBR. *J Appl Polym Sci* 13(4):797–805
- Sliozberg YR, Hoy RS, Mrozek RA (2014) Role of entanglements and bond scission in high strain-rate deformation of polymer gels. *Polymer* 55(10):2543–2551
- Jiang B, Zou Y, Liu T (2019) Characterization of the Fluidity of the Ultrasonic Plasticized Polymer Melt by Spiral Flow Testing under Micro-Scale. *Polymers* 11(2):357
- Pouchlý J (1970) Behavior of Macromolecules on the Phase Boundary. II. Conformational Statistics of the Linear Chain in a Pore. *J Chem Phys* 52(5):2567–2575

20. Duan T, Tang H, Liang R-Z (2019) Terminal group engineering for small-molecule donors boosts the performance of nonfullerene organic solar cells. *J Mater Chem A* 7(6):2541–2546
21. Koutsamanis I, Spoerk M, Arbeiter F (2020) Development of porous polyurethane implants manufactured via hot-melt extrusion. *Polymers* 12(12):2950
22. Xie H, Liu B, Chen H (2019) Inner relationship between the damping property and the sand-fixing durability of polymer materials. *J Appl Polym Sci* 136(11):47208
23. Li Z, Song S, Lv X (2021) Enhanced the melt strength, toughness and stiffness balance of the reactive PB-g-SAG core-shell particles modified polylactide blends with the aid of a multifunctional epoxy-based chain extender. *J Polym Res* 28(5):1–14
24. Luo Z, Sun R, Zhong C (2020) Altering alkyl-chains branching positions for boosting the performance of small-molecule acceptors for highly efficient nonfullerene organic solar cells. *Sci China: Chem* 63(3):361–369
25. Fu C-L, Ouyang W-Z, Sun Z-Y (2009) Solvent size effect on the static and dynamic properties of polymer chains in athermal solvents. *Polymer* 50(21):5142–5148
26. Boutaous M, h, Bourgin P, Zinet M, (2010) Thermally and flow induced crystallization of polymers at low shear rate. *J Nonnewton Fluid Mech* 165(5–6):227–237
27. Kim YC, Yang KS, Choi CH (1998) Study of the relationship between shear modification and melt fracture in extrusion of LDPE. *J Appl Polym Sci* 70(11):2187–2195
28. Gaillard A, Roché M, Lerouge S (2019) Viscoelastic liquid curtains: experimental results on the flow of a falling sheet of polymer solution. *J Fluid Mech* 873:358–409
29. Eceolaza S, Sangroniz A, del Río J (2019) Improving the barrier character of poly (caprolactone): Transport properties and free volume of immiscible blends. *J Appl Polym Sci* 136(40):48018
30. Davydova N, Mel'Nik V, Nelipovitch K (2002) The structural differences of benzophenone glasses according to different thermal history. *J Mol Struct* 614(1–3):173–176
31. Camillone N, Pak TR, Adib K (2006) Tuning Molecule– Surface Interactions with Sub-Nanometer-Thick Covalently Bound Organic Monolayers. *J Phys Chem B* 110(23):11334–11343

**Publisher's Note** Springer Nature remains neutral with regard to jurisdictional claims in published maps and institutional affiliations.